euronoise

Modelization of Acoustic Waves Radiation from Sources of Complex Geometry Aperture

Rafik Serhane and Tarek Boutkedjirt

Université des Sciences et de la Technologie Houari Boumediene; Faculté de Physique, BP 32, El-Alia, DZ-16111 Alger, Algeria
rafik_serhane@hotmail.com

Abstract - The Rayleigh integral giving the impulse response for the acoustic velocity potential cannot always be determined analytically for all types of transducer apertures. The shape of the transducer surface and the spatial distribution of the excitation on its surface can complicate the calculation. This makes using numerical methods indispensable. One of these methods consists in discretizing the aperture surface in polygonal shape elements.

Our work makes use of both methods of Jensen and Faure. In the former, the transducer surface is subdivided in triangles. The latter one uses additional virtual triangles one side of which is that of the physical element and its summit is the field point projection on the plane containing the considered physical element. Additionally, a rotation of the virtual triangle around the field point projection is performed. In this work, the orientations of those virtual triangles are considered according to Jensen method and their contributions to the impulse response are calculated according to the two situations described by Faure. The combination of the two methods is, then, generalized to the case of non planar complex surfaces such as concave phased arrays.

1 Introduction

The transmitting surface of an ultrasonic transducer can be considered as a set of point sources uniformly radiating in all directions. The radiated elementary wavelets propagate into the surrounding medium. At a point of this medium, the sound pressure field results from the superposition of the all these elementary contributions.

2 Pressure radiated by a mono-element planar transducer

The determination of the acoustic potential $\Phi(M,t)$ is based on the calculation of the Rayleigh integral, which is the mathematical formulation of the Huyghens-Fresnel principle [1,2]; that is :

$$\Phi(M,t)=\iint_{(S_0)} v_n(M_0,t)*\frac{\delta(t-R/c)}{2\pi R}\,dS_0, \qquad (1)$$

with $R=MM_0$. $\delta(t)$ is the Dirac impulse, $*$ the temporal convolution product, c propagation velocity of the ultrasonic wave in the considered medium and $v_n(M_0,t)$ the particle vibration velocity normal to the radiating surface. In the piston mode, this velocity has a uniform distribution on the surface (S_0). In this case, the vibration velocity depends only upon time $(v_n(M_0,t)=v_n(t).)$: The spatial impulse response for the acoustic potential $\Phi_i(M,t)$ is defined by:

$$\Phi_i(M,\ t)=\iint_{(s_0)}\frac{\delta(t-R/c)}{2\pi R}\ dS_0. \qquad (2)$$

This allows writing the acoustic potential at point *M*, which is referred by $\vec{r}$, by using a temporal convolution operation; that is :

$$\Phi(M,t)=v_n(t)*\Phi_i(\vec{r},t). \qquad (3)$$

As the acoustic pressure $p(M,t)$ and potential are related by :

$$p(M,t)=\rho\frac{\partial\Phi(\vec{r},t)}{\partial t}, \qquad (4)$$

where ρ is the equilibrium density of the propagating medium.

3 Method of discretizing the source surface

The triangles method (Fig. 1) has been proposed by two authors. Jensen [4] calculates the response by considering three geometric sub-triangles according to the field point position, each constituted by one side of the considered physical triangular element and the opposite summit, which is the projection of the field point on the plane containing the element surface (Fig 2). To calculate the response of each geometric sub-triangle, he applies to the latter a rotation around the projection of the field point so that one of its ridges is supported by the *Ox* axis. By using this procedure, the response of a sub-element is given according to five possible situations. Faure [5] considers sub-triangles one summit of which is the projection of the field point. The impulse response is calculated according to two possible situations (Fig. 3).
Our study makes use of both two methods. The orientations of the sub-triangles are considered by using the Jensen method and their contributions to the impulse responses for the potential are calculated according to the two situations considered by Faure (Fig. 3). Then the combination of the two methods is generalized to not planar complex surfaces.

3.1 Description of the method

One should first dispose of an analytic expression $(Z=f(X,Y))$, in the $(OXYZ)$ referential, of the geometric surface of the radiating aperture for which the impulse response is calculated. A mesh of the (XY) plane, which can be regular or not, causes discrete values at distance *Z*. Each set of coordinates (X_i,Y_i,Z_i) represents a knot of the mesh net, that is point A_i , which is the summit of an elementary polygon. In our case, the mesh is triangular, which corresponds to the simplest polygonal shape. It is constituted of three neighbouring knots of the mesh $(A_i,A_j,A_k)=(A,B,C)$ (Fig 1).

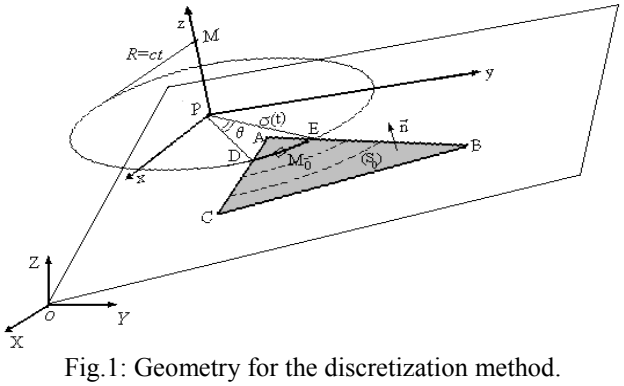

Fig.1: Geometry for the discretization method.

A so-called Delaunay triangularization function, which has been programmed under Matlab, furnishes directly the indices (i, j, k) of the three summits of each triangle lying on the surface. The spatial discretization interval is chosen sufficiently small so that the triangular element can be considered as planar. Each triangular element therefore defines a plane the normal to which is that of the triangle. As for planar surfaces, the impulse response for the acoustic potential is proportional to the angle subtended by the arc of circle, which is the intersection of the sphere of radius $R = ct$ and which is centered on the field point M, with the considered element (Fig.1). The intersection of the spherical wave front with the plane supporting this triangle is a circle of radius $\sigma(t) = \sqrt{c^2t^2 - z^2}$ and centered in *P*. *z* is the distance between the field point *M* and its projection *P* on the plane of the considered element. The determination of *z* requires the prior knowledge of the equation of the plane containing the considered element. This equation has the following form :

$$\alpha X + \beta Y + \gamma Z + \delta = 0. \qquad (5)$$

Let *N(X,Y,Z)* an arbitrary point of the plane containing the triangular element *ABC*. The coordinates of points *A, B* and *C* verify the equation (6) of the plane. This permits relating the constants α, β, γ and δ to these coordinates by :

$$\begin{cases} \alpha = Y_B Z_C - Z_B Y_C \\ \beta = Z_B X_C - X_B Z_C \\ \gamma = X_B Y_C - Y_B X_C \\ \delta = -(\alpha X_A + \beta Y_A + \gamma Z_A) \end{cases} . \qquad (6)$$

We deduce then the vector $\vec{n}$, which is normal to the plane of the element; that is: $\vec{n}(\alpha, \beta, \gamma)$. Point $P(X_P, Y_P, Z_P)$ is the projection of the field point $M(X_M, Y_M, Z_M)$ on this plane. *P* and *M* must verify $\vec{PM} = \xi\vec{n}$, where ξ is a proportionality factor, therefore :

$$\begin{cases} X_P = X_M - \xi\alpha \\ Y_P = Y_M - \xi\beta \\ Z_P = Z_M - \xi\gamma \end{cases} . \qquad (7)$$

The coordinates of point *P* verify the plane equation to which it belongs :

$$\alpha X_P + \beta Y_P + \gamma Z_P + \delta = 0. \qquad (8)$$

If in addition, we take account of the equations system (7), we obtain the proportionality factor ξ :

$$\xi = \frac{\alpha X_M + \beta Y_M + \gamma Z_M + \delta}{\alpha^2 + \beta^2 + \gamma^2}. \qquad (9)$$

By replacing ξ in the precedent system (7), the coordinates of *P* can be deduced. The distance *PM=z* is :

$$z = \sqrt{(X_P - X_M)^2 + (Y_P - Y_M)^2 + (Z_P - Z_M)^2}. \qquad (10)$$

Let us consider the active triangular element *ABC* of this set (taken alone in Fig. 2). To calculate the impulse response of this element, we should consider the projection *P* of the field point as the origin of the new referential *(Pxyz),* so that the plane *(x,y)* be the element plane. Consequently, a change of the origin and of the axes orientation is performed. All the coordinates are then expressed in the new referential *(Pxyz)*.

To determine the impulse response for the acoustic potential of element *ABC* which is denoted by *m,* we should consider the three sub-triangles *PAB*, *PAC* and *PBC* (Fig.2). The response of the element is the sum of three responses, each with a contribution sign, according to the orientation of its corresponding sub-triangle; that is :

$$\phi_{ie}^{m}(M,t) = \sum_{k=1}^{k_{\max}} s_k h_{ik}(M,t). \qquad (11)$$

$k_{\max} = 3$ and h_{ik} is the impulse response of the k^{th} triangular sub-element contributing to the physical element response with the sign $s_k = \pm 1$.

For the signs of the sub-triangles contributions, three cases are possible. These are illustrated in Fig.2. If the projection *P* of the field point *M* is situated inside element *ABC,* then the signs of the contributions are all positive. If not, the observer which is placed in *P* sees the triangle *ABC* under angle Φ. The nearest sub-triangles formed by the sides of element *ABC* and *P* contribute with a negative sign (*PAB* and *PAC* (Fig 2.b) and *PAC* (Fig 2.c)). All others have positive contributions.

To mathematically determine if the projection *P* of the field point is situated on the radiating surface *ABC* or not, it is sufficient to draw a straight line from *P* that crosses one side of triangle *ABC* in *Q*. It should necessarily cross an

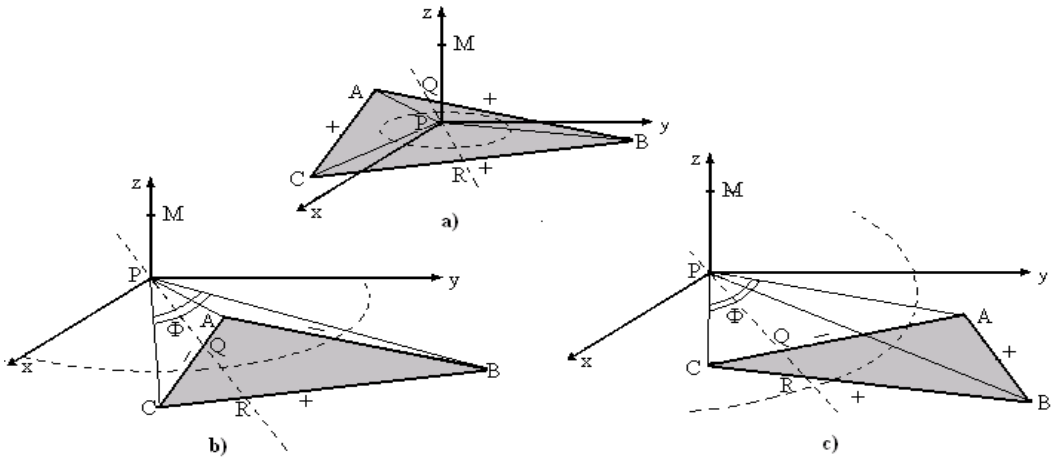

Orientation: a) $\phi_{i\,ABC} = \phi_{i\,PAB} + \phi_{i\,PBC} + \phi_{i\,PCA}$
b) $\phi_{i\,ABC} = -\phi_{i\,PAB} + \phi_{i\,PBC} - \phi_{i\,PCA}$
c) $\phi_{i\,ABC} = \phi_{i\,PAB} + \phi_{i\,PBC} - \phi_{i\,PCA}$

Fig. 2: Geometry for the determination of the sign of the sub-elements contribution to the impulse response of the triangular element.

other side in R.. The negative scalar product $\vec{PQ}.\vec{PR}$ signifies that point P is inside the element and all other contributions are positive (Fig 2.a). If not, it is outside the element. In this second case, $(\vec{PQ}.\vec{PR} \geq 0)$. If in addition $\overline{PQ} < \overline{PR}$ (Fig. 2.b et 2.c), then the sub-triangle formed by point P and the side going through R contributes with a positive sign. The other sub-triangle, formed by point P and the side containing Q, contributes with a negative sign. Otherwise $(\overline{PR} < \overline{PQ})$, the sign of the sub-elements contributions is inverted.

3.2 Sub-element and element responses

The determination of the impulse response of a sub-element requires the calculation of the contribution angle $\theta(M,t)$, so that:

$$h_{ik}(M,t) = \frac{c}{2\pi}\theta_k(M,t). \qquad (12)$$

Let us consider the sub-element PAB situated in referential $(Pxyz)$ which is relative to element ABC (Fig 3).

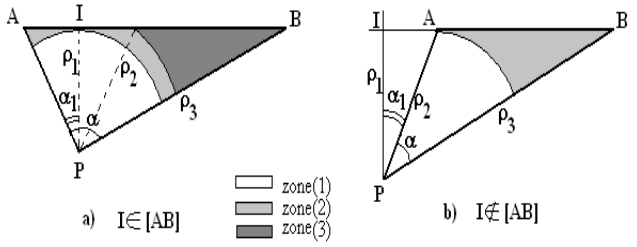

Fig. 3: Geometry for the determination of the sub-element impulse response.

The equation of the straight line (AB) is given by [5] :

$$y = m_0 x + y_0. \qquad (13)$$

The constants m_0 and y_0 are function of A and B coordinates :

$$m_0 = \frac{y_B - y_A}{x_B - x_A} \quad and \quad y_0 = y_A - (\frac{y_B - y_A}{x_B - x_A})x_A. \qquad (14)$$

Let I be the projection of point P on the straight line (AB). Two cases can be distinguished: I belongs to segment $[AB]$ or not, according to the position of P. We define, then, ρ_1 as the distance between P and the straight line (AB); that is:

$$\rho_1 = \frac{y_0}{\sqrt{1+m}}. \qquad (15)$$

ρ_2 and ρ_3 are the minimal and the maximal distance from A or B to P respectively :

$$\rho_2 = \min(\overline{PA}, \overline{PB}) = \min(\sqrt{x_A^2 + y_A^2}, \sqrt{x_B^2 + y_B^2}),$$
$$\rho_3 = \max(\overline{PA}, \overline{PB}) = \max(\sqrt{x_A^2 + y_A^2}, \sqrt{x_B^2 + y_B^2}). \qquad (16)$$

The distances from the field point to the different positions of discontinuities with the sub-element sides are given by :

$$r_i = \sqrt{z^2 + \rho_i^2}, \quad i = 0,..,3, \qquad \text{with :} \quad \rho_0 = 0.$$

The corresponding instants are:

$$\tau_i = r_i / c. \qquad (17)$$

The angles α et α_1 represented in Fig.3 are given by :

$$\alpha = \tan^{-1}(\frac{x_A}{y_A}) - \tan^{-1}(\frac{x_B}{y_B}) \qquad (18)$$

and

$$\alpha_1 = \cos^{-1}(\frac{\rho_1}{\rho_2}). \qquad (19)$$

The response of the k^{th} sub-element $(1 \leq k \leq 3)$ is :

$$h_{ik} = \begin{cases} 0 & \text{if} \quad t \leq \tau_0 \\ \dfrac{c\alpha}{2\pi} & \text{if} \quad \tau_0 \leq t \leq \tau_1 \\ \dfrac{c}{2\pi}(\alpha - 2.\arccos(\dfrac{\rho_1}{\sigma(t)})) & \text{if} \quad \tau_1 \leq t \leq \tau_2 \\ \dfrac{c}{2\pi}(\alpha - \alpha_1 - \arccos(\dfrac{\rho_1}{\sigma(t)})) & \text{if} \quad \tau_2 \leq t \leq \tau_3 \\ 0 & \text{if} \quad t \leq \tau_3 \end{cases} \text{ if } I \in [AB],$$

and

$$h_{ik} = \begin{cases} 0 & \text{if} \quad t \leq \tau_0 \\ \dfrac{c}{2\pi}\alpha & \text{if} \quad \tau_0 \leq t \leq \tau_2 \\ \dfrac{c}{2\pi}(\alpha + \alpha_1 - \arccos(\dfrac{\rho_1}{\sigma(t)})) & \text{if} \quad \tau_2 \leq t \leq \tau_3 \\ 0 & \text{if} \quad t \leq \tau_3 \end{cases} \text{ if } I \notin [AB],$$

with

$$\sigma(t) = \sqrt{c^2 t^2 - z^2}. \qquad (20)$$

A summation on the three sub-triangles $(k_{\max} = 3)$ of the considered ABC element furnishes the impulse response of that element.

This impulse response is represented in Fig. 4.a for different positions of the field point projection on the plane of the element. These projections are illustrated in Fig. 4.b. It should be noticed that, every time the spherical wave encounter an edge of the triangular element, the spatial impulse response shows an important variation at the corresponding instant. The number of these discontinuities depends on the field point position.

The total impulse response of the transducer is obtained by summing the impulse responses of each elements; that is :

$$\phi_{ie}(M,t) = \sum_{m=1}^{M} \phi_{ie}^m(M,t), \qquad (21)$$

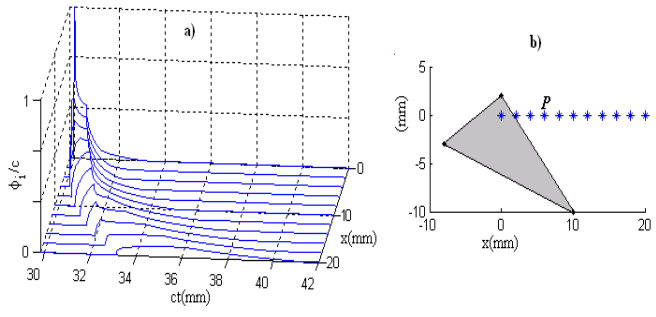

Fig 4 a) Impulse response for the velocity potential of a triangular element represented in b) for different positions of the field point on the x axis (y=0) and at plane z=30 mm

The efficiency of this method for such geometries depends on its precision and the calculation time of the response. In order to reduce the error risk and to optimize the method, it is first tested in the case that an analytic expression of the impulse response is available.

4 Discretization method applied to a circular focusing transducer

The surface of a circular focusing transducer is subdivided in a number N of triangular elements (Fig. 5) so that each element can be considered as planar and the mesh method previously described can be applied.
Let us consider a circular focusing transducer of radius $a = 10$ mm, of focal distance $F = 50$ mm and which is discretized in 5584 triangular elements.

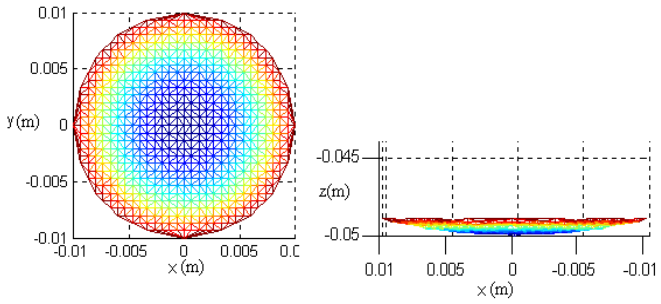

Fig. 5: Mesh of a circular focusing transducer.

The spatial impulse response for the acoustic potential of this transducer though calculated at the field point of coordinates (x=1mm, y=0, z=20mm, relatively to the focus chosen as origin) shows an average error of 3.5 % relatively to the results given by the analytic method [6,7] (Fig 6). This relative difference between the impulse responses obtained by the two methods is given by :

$$\frac{\Delta\phi_i}{\phi_i} = \frac{\phi_i(\text{analytic}) - \phi_i(\text{discretized})}{\phi_i(\text{analytic})}$$

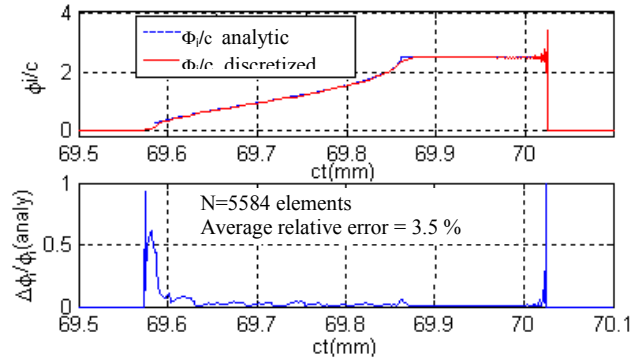

Fig.6 : Impulse responses calculated by the two methods for N= 5584 elements at x= 1 mm, z=20 mm.

It can be noticed that the relative error is negligible in the time interval corresponding to the direct wave regime although the transmitting surface is curved. The relative error is maximal at the discontinuities instants of the impulse response.

5 Generalization of the mesh method to a curved rectangular transducer (cylindrical)

The application of the discretization method to surfaces for which an analytic expression of the impulse response is available has permitted testing its efficiency in order to be generalized to more complex geometry surfaces.
A curved rectangular transducer of dimensions ($2a = 6$ mm, $2b = 20$ mm), of curvature radius $R = 20$ mm (depth $e = 2,68$ mm) is represented in Fig. 7. Such transducers are generally used as elements of a linear

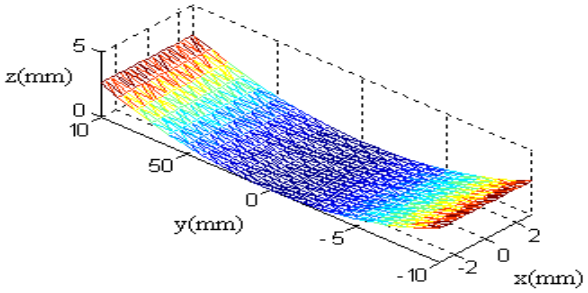

Fig. 7 : Curved rectangular transducer of dimensions ($2a$=6mm, $2b$=20 mm) and curvature radius R=20 mm, discretized in 5000 triangular elements.

transducers array in order to reduce the focus width along (Oy).
In the focal plane (z=20 mm), the response is maximal for a field point the projection of which is situated on the radiating surface ($|x| \le 3$ mm and y=0). These positions correspond to a segment describing the focal zone. In the same region, the pressure field (Fig 8.a) is composed of a direct wave component ("plane") followed by an edge wave component of lower amplitude. These two contributions interfere because of the excitation duration which is represented in Fig. (8.d). The direct wave component is proportional to the source acceleration. Far from the axis (at $x = 2$ mm) and being on the segment of the straight line defining the focal zone, the edge wave component appears. Its destructive interference with the "plane "wave furnishes an amplitude lower than that obtained on axis ($x = 0$). At greater distances from the axis (Oz) ($x \ge 3$ mm), the field point is no more in the focal zone and the response for the potential becomes "flat". Only the transducer edges contribute to the pressure field with two replicas of inverse polarities. The "plane" wave regime for which the response stay maximal and constant is obtained for ($|x| < a$). The pressure field is composed of a "plane" wave which has the form of the excitation (Fig 8.b) followed by two edge waves components. In the shadow zone ($|x| \ge a$), the pressure field is constituted of two edge waves components of very low amplitude, which become more time separated when x increases.

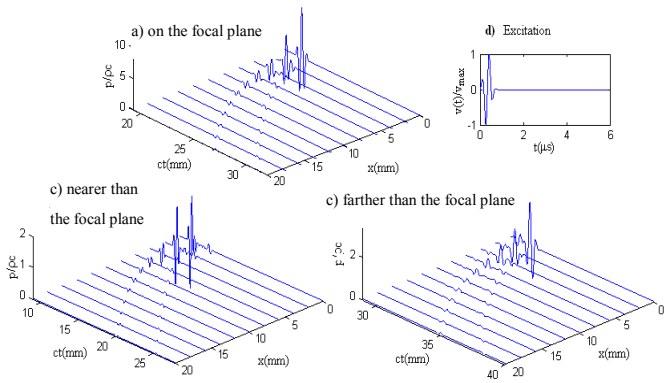

Fig. 8 : Pressure radiated by a curved rectangular transducer for different positions x of the field point : a) in the focal plane (z = 20 mm), b) nearer than focal plane (z=10mm), c) farther than the focal plane (z = 30 mm) and d) Excitation waveform.

Farther than the focus, the field point receives first the contributions of the nearest transducer edges. If the field point has a projection on the radiating surface ($|x| \le 3$

mm), then, during a very short time interval, a "plane" wave regime appears (Fig 8.c). The "plane" wave component has an inverse polarity relatively to the excitation and is preceded by an edge wave of lower amplitude and of the same polarity as the excitation (Fig.8.c).

Out of axis, the response for the acoustic potential has a monotone increasing regime then it decreases before it nullifies. The greater the radial distance x, the greater the duration of the decreasing regime is. In addition, only two edge wave components constitute the pressure field.

6 Concave linear array

The discretization method previously described can be generalized to calculate the field of a concave array.

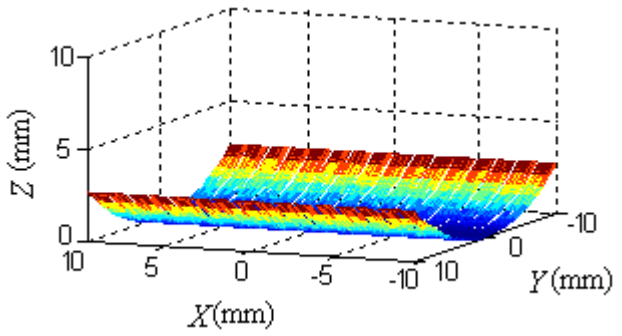

Fig. 9 : Linear concave array : N = 16 elements, 2a=1mm, 2b=20 mm, d=1.2 mm and R=20 mm.

The transducer represented in Fig. 9 figure is constituted of 16 mono-elements of dimensions (2a=1 mm, 2b=20 mm) and which are aligned along the (Ox) axis. The distance between the centers of two successive elements is d=1.2 mm and the curvature radius is R=20 mm.
The impulse responses for the acoustic potential of the elements for a simultaneous excitation of the elements are represented in Fig.10.
A field point on the axis (x=0, y=0, z=20 mm) receives first the wavelets issued from the two central elements. The superposition of the responses of two symmetric elements furnishes a response of double amplitude and the responses of successive elements start at separated times. These results are comparable to those given by [8].

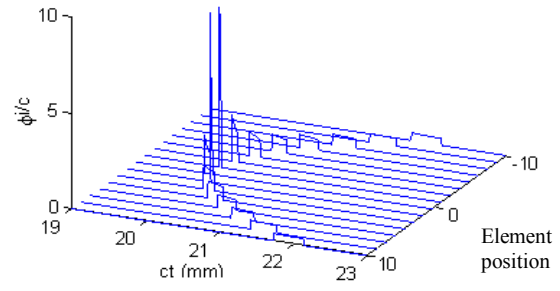

Fig. 10 : Individual impulse responses for the acoustic potential of a concave array obtained by the discretization method

7 Effect of the mesh elements number

For $N \geq 5000$, the relative error becomes negligible and nearly constant (Fig. 11.a). The calculation time varies "linearly" with N (Fig 11.b). By limiting N around 2500, the calculation time stays reasonable (in the order of 35 s on an Intel Celerone 1GHz personal computer) and the relative error is acceptable (in the order of 3.5%).

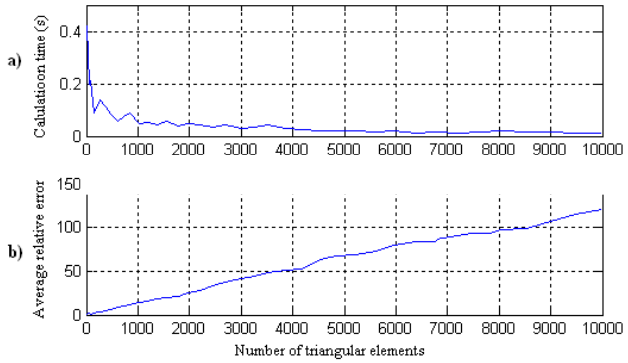

Fig. 11 : Effect of the number of mesh elements N a) on the average relative error and, b) on the calculation time of the impulse response by using the discretization method.

8 Conclusion

The described method which uses triangles formed by the edges of the mesh elements can be generalized to any geometry of the mesh element. It is sufficient that this geometry is polygonal. In this case, the summation of the contributions of the triangular sub-elements above defined furnishes the impulse response of the element considered (Eq. 11), with k_{max} being the number of sides constituting the elementary polygon. The efficiency of this method for such geometries depends upon its precision and the calculation time of the response. To reduce the error risk and optimise the method, the latter has been first tested in the case that an analytic expression of the impulse response is available. This combination has permitted to generalize the mesh method to any type of radiating surface.

References

[1] P. R. Stepanishen, "Transient radiation from pistons in an infinite planar baffle", *J. Acoust. Soc. Am.* 49(5) 1628-1638 (1971)

[2] G.R. Harris, "Transient field of a baffled planar piston having an arbitrary vibration amplitude distribution", *J. Acoust. Soc. Am.* 71(1) 186-204 (1981)

[3] J. A. Jensen and N. B. Svendsen, "Calculation of pressure fields from arbitrarily shaped, apodized and excited ultrasound transducers," *IEEE Trans. Ultrason. Ferroelect. Freq. Contr.* 39(2) 262-266 (1992)

[4] J. A. Jensen, "Ultrasound fields from triangular apertures", *J. Acoust. Soc. Am.* 100(4) 2049-2056 (1996)

[5] P. Faure, D. Cathignol and J. Y. Chapelon, "Diffraction impulse response of arbitrary polygonal planar transducers", *Acta Acustica.* 2 257-263 (1994)

[6] H. Djelouah : Contribution à l'étude du rayonnement des champs ultrasonores impulsionels dans les liquides et les solides. *Thèse de Doctorat d'Etat, U.S.T.H.B., Alger* (1990).

[7] H. T. O'Neil, "Theory of focusing radiators", *J. Acoust. Soc. Am.* 21(5) 516-526 (1949)

[8] W. Ping, "Spatial impulse response method for predicting pulse-echo field from a linear array with cylindrically concave surface", *IEEE Trans. Ultrason. Ferroelect. Freq. Contr.* 46(5) 1283-1297 (1999).